

Research Article

STRUCTURAL AND MAGNETIC PROPERTIES OF Cr³⁺ SUBSTITUTED NICKEL FERRITE NANOPARTICLES

B.H. DEVMUNDE*, M.B.SOLUNKE

Vivekanand Arts S.D. Comm & Sci. College, Aurangabad. Vasantrao Naik College, Aurangabad. Email: bhdevmunde05@gmail.com,

Received: 17 March 2020, Revised and Accepted: 05 April 2020

ABSTRACT

Objective: The nickel ferrite is promising magnetic material and has several applications; ranging from radio frequency and microwave frequency. They can be used in transformers, inductors, antenna rods, memory chip etc. Recently they have found applications in sensors, green anode materials and drug delivery.

Materials and Methods: A nominal composition of NiCr_xFe_{2-2x}O₄ with x varying (0.0, 0.1, 0.2, 0.3, 0.4, 0.5 and 0.6) has been prepared by Sol-Gel auto-combustion method.

Chemicals such as nickel nitrate hexahydrate, Chromium nitrate nonahydrate, ferric nitrate nonahydrate and Dextrose used as fuel. Ammonia solution was added to maintain pH 7. synthesis powder is sintered at 750 °C for 6 hours.

Results: XRD for all samples recorded at room temperature model (3710) using Cu-Kα radiation (λ=1.5406 Å). Infrared (IR) spectra were recorded using Fourier transform infrared spectrometer (Perkin Elmer Instruments USA) in range 1000-370cm⁻¹ with resolution 1 cm⁻¹. Magnetic properties of nanoparticles were performed using pulse field hysteresis loop, XRD pattern shows broad peaks. IR spectra confirmed spinel cubic structure, saturation magnetization, remanence magnetization, coercivity decreases with increase in chromium substitution.

Conclusion: Using sol-gel method the particle size of about 15-33 nm was achieved. The obtained values of coercivity revealed that the prepared samples possess nano-crystalline nature.

Keywords: - Nickel ferrite, sol gel method, Magnetic properties, XRD

INTRODUCTION

Various trivalent metal ions like Al³⁺, Cr³⁺, Ho³⁺ were substituted in spinel ferrite and metal oxide [1-3]. Recently it has been recognized that substituting Cr³⁺ into TiO₂ could affect growth of grains [4] due to predominantly the large difference in valence band structure Cr³⁺ & Ti⁴⁺. A high substituting content of Cr³⁺ will break the anatase structure of TiO₂ and enable the formation of rutile structure in the resultant particle for this reason the substituting content of Cr³⁺ is usually less than 3.8% (Molar percent with respect to Ti) which means the controllable range of size is quite limited and narrow. Nickel and Cr³⁺ substituted nickel ferrite is one of the versatile and technologically important soft ferrite materials because of its typical ferromagnetic properties, low conductivity and thus eddy-current losses, high electrochemical stability, catalytic behavior, abundance in nature [5, 6, 7].

EXPERIMENTAL DETAILS

Synthesis of NiCr_xFe_{2-2x}O₄ nanoparticles

A nominal composition of NiCr_xFe_{2-2x}O₄ with composition x (where x = 0.0, 0.1, 0.2, 0.3, 0.4, 0.5 and 0.6) has been prepared by sol-gel auto combustion method. AR grade chemical such as nickel nitrate hexahydrate (Ni(NO₃)₂·6H₂O), chromium nitrate nonahydrate (Cr(NO₃)₃·9H₂O), ferric nitrate nonahydrate (Fe(NO₃)₃·9H₂O) and dextrose (C₆H₁₂O₆) were used as a fuel for the synthesis. All the chemicals used for the synthesis were analytical grade. Dextrose was used as a fuel. The metal nitrates to fuel (dextrose) ratio was taken as 1:1.66. Ammonia solution was added to maintain the pH 7. The temperature required for the synthesis of Ni-Cr ferrite nanoparticles was low that is around 120 °C. The as-synthesized powder is sintered at 750 °C for 6 hours.

RESULT AND DISCUSSION

X-ray diffraction (XRD)

Structural studies of NiCr_xFe_{2-2x}O₄ (with 0.0, 0.1, 0.2, 0.3, 0.4, 0.5 and 0.6) ferrite nanoparticles under investigation were carried out using X-ray diffraction technique. All the samples under study exhibit single phase cubic spinel structure without any secondary peaks (fig. a, b, c.) depicts the X-ray diffraction pattern of the present samples.

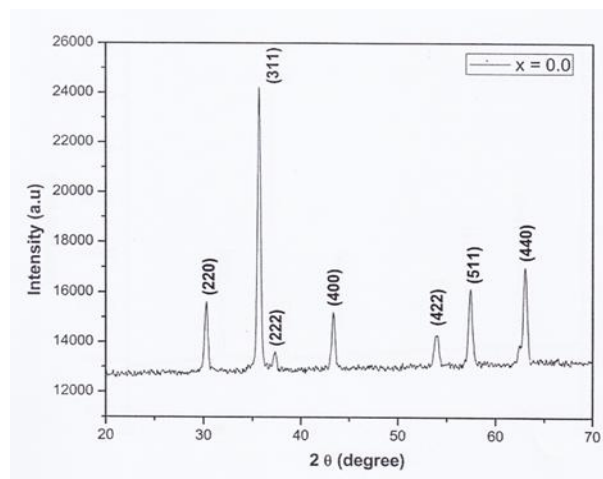


Fig. a: X ray diffraction pattern of NiCr_xFe_{2-2x}O₄ system for [x=0.0]

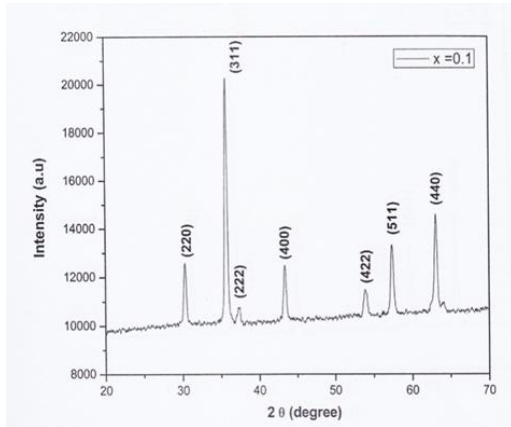


Fig. b: X ray diffraction pattern of NiCr_xFe_{2-2x}O₄ system for[x=0.1]

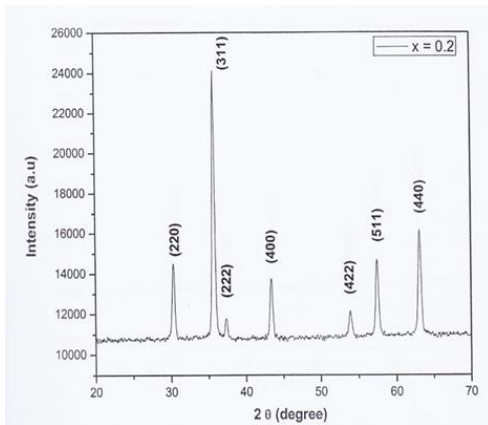


Fig. c: X ray diffraction pattern of NiCr_xFe_{2-2x}O₄ system for[x=0.2]

The XRD pattern confirms the formation of single-phase cubic spinel structure as the corresponding planes such as (220), (311), (222), (400), (422), (511) and (440) are present in it. Various crystalline parameters like interplanar spacing (d), X-ray density (d_x), lattice constant (a), unit cell volume (V), average crystalline sizes (t) etc have been calculated from XRD data. Table 1.1 Lattice constant (a), X-ray density (d_x) volume of unit cell (V) and crystallite size (t) of NiCr_xFe_{2-2x}O₄

Table 1.1: Lattice constant [a],X-ray density[dx],Volume of unit cell[V],Crystallite size [t] for sample of NiCr_xFe_{2-2x}O₄ system.

'x'	Lattice Constant (Å)	X-ray density (gm/cm ³)	Volume (Å) ³	Crystallite (nm)
0.0	8.3345	5.3781	578.95	33.55
0.1	8.3311	5.2474	578.25	30.78
0.2	8.3164	5.1374	575.19	28.62
0.3	8.2920	5.0439	570.13	24.77
0.4	8.2830	4.9208	568.28	18.93
0.5	8.2706	4.8028	565.73	17.59
0.6	8.2609	4.6789	563.75	15.55

IR Spectra

Fig. (d, e, f,) depicts the IR spectra for typical sample NiCr_xFe_{2-2x}O₄ (X=0.0, 0.1 and 0.2) Two prominent absorption bands are seen in their spectra which looks different than their spectra of bulk samples. The major absorption bands are found to be broad which is attributed to smaller particle dimensions of samples [8-10]

Magnetic properties

Pulse filled hysteresis loop technique measurement

Magnetization of ferrites is influenced by several intrinsic and extrinsic factors such as density, anisotropy, grain size and A-B exchange interaction. The plots of magnetization versus applied field

(M-H) helps in understanding the magnetic response of material and provides the useful information about the magnetic parameters such as saturation magnetization (M_s), Coercivity (H_c) remanence magnetization (M_r) and magneton number. The hysteresis plots (M-H) of NiCr_xFe_{2-2x}O₄ nanoparticles and are depicted in Fig. (g, h, i, j). The magnetic parameters were obtained using magnetization curve and are shown in Table 1.2 The variation of saturation magnetization values with chromium content are shown Table 1.2 . The saturation magnetization decreases with chromium content.

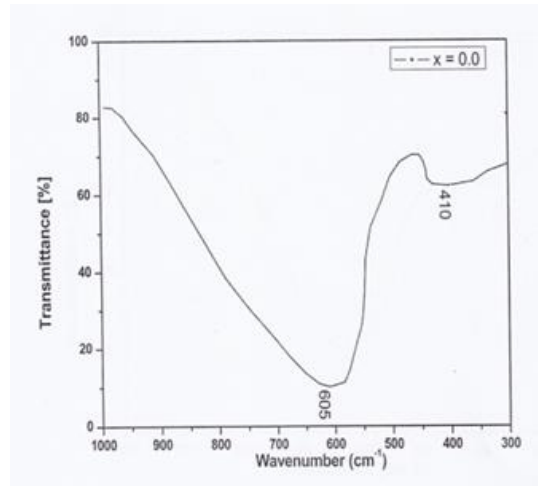


Fig. d: The IR spectra for the sample [x=0.0] of the system NiCr_xFe_{2-2x}O₄

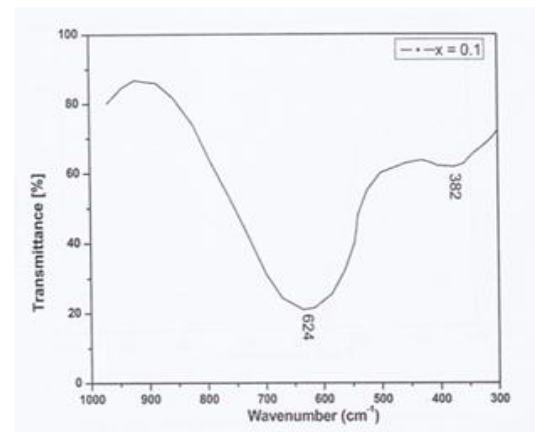


Fig. e: The IR spectra for the sample [x=0.1] of the system NiCr_xFe_{2-2x}O₄

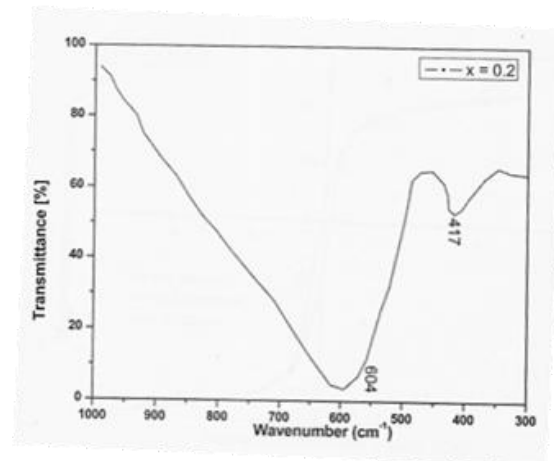


Fig. f: The IR spectra for the sample [x=0.2] of the system NiCr_xFe_{2-2x}O₄

Table 1.2: Saturation magnetization[Ms], Remanance magnetization [Mr], Coercivity[Hc] and Magneton number[N_B] for sample of NiCr_xFe_{2-2x}O₄ system.

'x' mol	Ms (emu/g)	Mr (emu/g)	Hc (Oe)	Mr/Ms	N _B (μ _B)
0.0	46.12	14.27	165	0.309	1.935
0.1	61.83	19.26	143	0.311	2.529
0.2	57.08	18.11	142	0.317	2.273
0.3	53.37	16.72	124	0.313	2.069
0.4	52.01	12.21	110	0.235	1.960
0.5	38.14	10.32	108	0.271	1.397

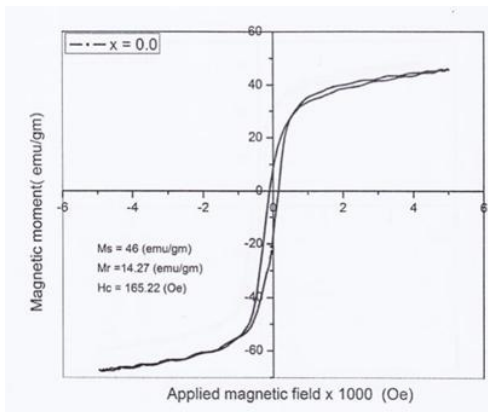


Fig. g: The Hysteresis plots [M-H] for[x=0.0]

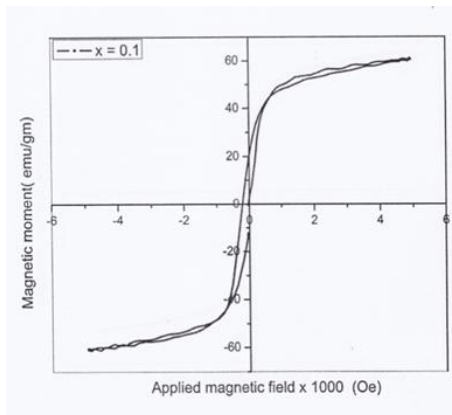


Fig. h: The Hysteresis plots [M-H] for[x=0.1]

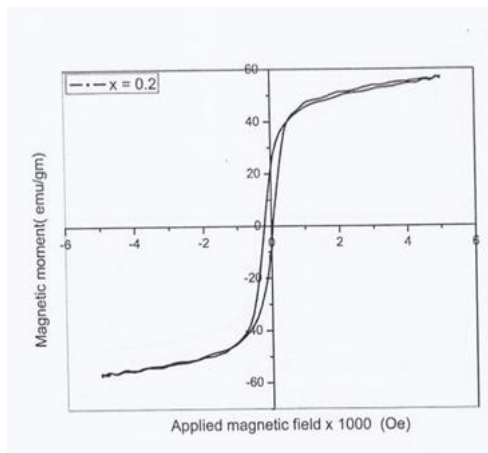


Fig. i: The Hysteresis plots [M-H] for[x=0.2]

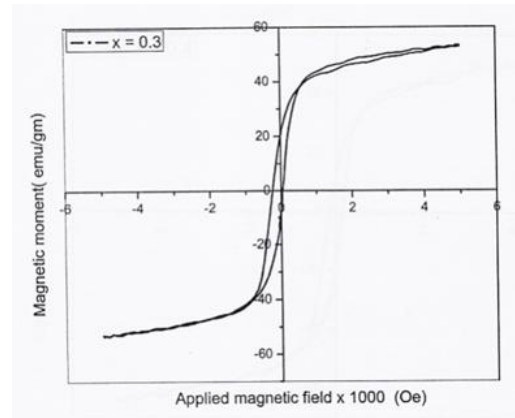


Fig. j: The Hysteresis plots [M-H] for[x=0.3]

The Hysteresis Plots (M-H) of NiCr_xFe_{2-2x}O₄

CONCLUSIONS

The following conclusion can be drawn from the present study; the samples of NiCr_xFe_{2-2x}O₄ were successfully synthesized by Sol-gel auto combustion method. XRD patterns show broad bragg's peaks. The lattice parameter decreases with increase chromium content in nickel ferrite. The two broad absorption bands are seen in IR spectra which confirmed spinel cubic structure. Using Sol-gel method the particle size of about 15-33 nm was achieved. Saturation magnetization, remanance magnetization, coercivity decreases with increase in chromium substitution. The obtained values of coercivity revealed that the prepared samples possess nanocrystalline nature.

REFERENCES

1. Kubo, O.; T.; Yokoyama, H., IEEE Transactions on Magnetics 1982, 18(6), 1122-1124.
2. Chu, Y.-Q.; Fu, Z.W.; Qin, Q.-Z., Electrochimica Acta 2004, 47(27), 4915-4921.
3. Charles, D.D.; Martin, J., Method for producing zinc ferrite pigment. Google Patents: 1959.
4. Schloemann, E., Journal of magnetism and magnetic Materials 2000, 209(1), 15-20.
5. Stoppels, D., Journal of Magnetism and Magnetic Materials 1996, 160, 323-328.
6. King, J.S., Ferrite rod antenna. Google patents: 1991.
7. Dee, R.H.; Cates, J.C., Magnetic tape head assembly having segmented heads. Google Patents: 2000.
8. Vestal, C.R.; Zhang, Z.J., Journal of the American Chemical Society 2003, 125(32), 9828-9833.
9. Yan, C.-H.; Xu, Z.-G.; Cheng, F.-X.; Wang, Z.-M.; Sun, L.-D.; Liao, C.-S.; Jia, J.-T., Solid State Communications 1999, 111(5), 287-291.
10. Ayyappan, S.; Mahadevan, S.; Chandramohan, P.; Srinivasan, M.; Philip, J.; Raj, B., The journal of Physical Chemistry C 2010, 114(14), 6334-6341.
11. Gangopadhyay, S.; Hadjipanayis, G.; Dale, B.; Sorensen, C.; Kalbunde, K.; Papaefthymiou, V.; Kostikas, A., Physical Review B 1992, 45(17), 9778.
12. VanEsch, A.; Van Bockstal, L.; De Boeck, J.; Verbanck, G.; Van Steenberghe, A.; Wellmann, P.; Grietens, B.; Bogaerts, R.; Herlach, F.; Borghs, G., Physical Review B 1997, 56(20), 13103.
13. Frankmp, B.L.; Boal, A.K.; Tuominen, M.T.; Rotello, V.M., Journal of the American Chemical Society 2005, 127(27), 9731-9735.